J. Korean Math. Soc. **42** (2005), No. 4, pp. 827–845

STABILITY ANALYSIS OF BURSTING MODELS

EUIWOO LEE

ABSTRACT. In this paper, we present a general method for the stability analysis of some bursting models. Our method is geometric in the sense that we consider a flow-defined return map defined on a section and determine when the map is a contraction. We find that there are three different stability types in the codimension-1 planar bursters.

1. Introduction

The term *bursting* refers to the dynamic activity in which some variables undergo alternations between an active phase of rapid, spike-like oscillations and a silent phase of near steady state resting behavior as shown in Fig 1. This activity is observed in various electrically excitable biological systems such as nerve cells, secretory cells, and muscle fibers ([1, 4, 6, 16, 18, 22]).

There are several different classes of bursting oscillations and there have been considerable efforts in trying to formulate and classify the underlying mechanisms responsible for these oscillations ([3, 7, 19, 20]). For comprehensive reviews, see [12, 21]. Most of the mathematical models for bursting oscillations are based on the observation that the systems contain variables of significantly different time scales, so they are described by slow-fast systems. This often leads to interesting mathematical issues in the theory of singular perturbations and bifurcation problems ([9, 11, 13, 17, 23, 24]).

In this paper we develop a general method for the stability analysis of bursting models, which can be applied to a large class of bursters. For the stability analysis of some of the specific models, see [8, 15]. Our general approach is straightforward. We construct a section transverse

Received June 2, 2004.

2000 Mathematics Subject Classification: 34D15, 34C23, 92B05.

Key words and phrases: bursting, stability, bifurcation, delayed behavior, singular perturbation.

This work was supported by the Soongsil University Research Fund.

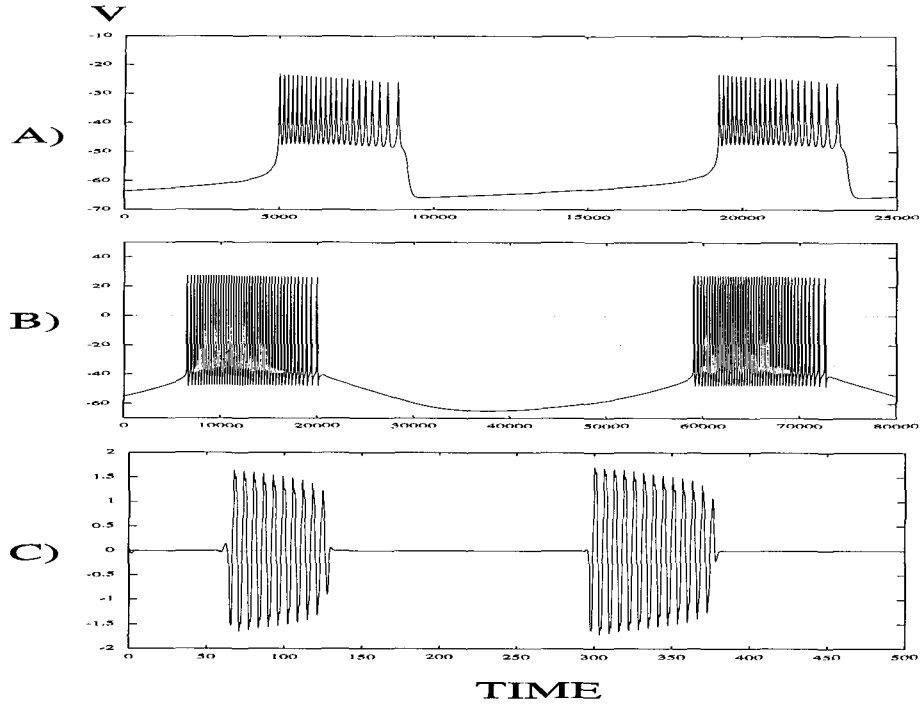

FIGURE 1. Examples of bursting solutions. A: square-wave bursting, B: parabolic bursting, C: elliptic bursting.

to the flow and determine when the Poincaré return map on the section becomes a contraction. To analyze the return map, we divide it into a few different pieces and consider each piece. From our stability analysis, we find that the primary factor which contributes to the instabilities of some of the codimension-1 planar bursters is the delayed behavior in the transitions between the steady states and the oscillatory states. Analyzing different delayed behaviors, we also show that there are three different stability types in the bursters.

The present article is organized in the following order. In Section 2, a general mathematical mechanism of bursting activities is explained. In Section 3, we give some examples of different bursting models and introduce a classification scheme of codimension-1 planar bursters. Section 4 contains the main body of the mathematical results for our stability analysis. The main result is stated in the final section, where we also discuss some of the related issues.

2. Bursting mechanisms

The mathematical theory for the analysis of bursting models is based on the observation that these models contain variables of significantly different time scales. In the case of electrical activities of excitable membrane systems, bursting occurs on the time scale of seconds, while the spiking has time scale of milliseconds.

We consider systems of the form

$$\begin{cases} \dot{x} &= f(x,y) \\ \dot{y} &= \epsilon g(x,y), \end{cases} \tag{2.1}$$

where $x \in \mathbf{R}^n$ and $y \in \mathbf{R}^m$ are fast and slow variables, and $\epsilon > 0$ is a small parameter representing the ratio of two different time scales.

If $\epsilon = 0$, then y is a constant, and we can consider y to be a parameter in the first equation of (2.1):

$$\dot{x} = f(x,y). \tag{2.2}$$

We refer to (2.2) as the fast subsystem (FS) and the second equation of (2.1) as the slow system.

In the analysis of the system (2.1), we first analyze (FS) and determine the attracting sets of (FS), which mainly include fixed points and periodic solutions. Next, we superimpose slow dynamics onto the fast subsystem to see how the trajectories of the full system move around the attracting sets.

In the bursting model, the trajectories move periodically between a branch of periodic solutions and a branch of fixed points which correspond to the active phase of repetitive spiking and the silent phase of near steady state behavior respectively. The abrupt transitions between the steady state and repetitive spiking occur near the bifurcations of (FS). In the transitions, there are several different bifurcation structures, which basically determine different bursting patterns.

3. Examples of different bursters

In this section we present a classification scheme for bursting oscillation. The scheme is based on the different bifurcation structures in the transitions between steady states and oscillatory states. We first describe three different types of bursting oscillations proposed by Rinzel [19].

3.1. Square-wave bursting

The transition from steady state to oscillatory state occurs through a saddle-node bifurcation, and the spiking terminates at a homoclinic bifurcation as shown in Fig 2.A. We need to hypothesize that $\dot{y} > 0$ near the lower branch of stable fixed points and $\dot{y} < 0$ near the upper branch of stable limit cycles. In this case, the repetitive alternations between the steady states and the oscillatory states occur through a hysteresis loop. Since the active phase terminates via a homoclinic bifurcation, the spiking frequency decreases at the end of the active phase. See Fig 1.A.

Square-wave bursting is observed in the model for electrical activities in pancreatic β-cell ([5, 22]) and models of respiratory rhythm generation in the pre-BötC complex ([4]). The following system of differential equations give rise to square-wave bursting ([10]).

$$\left\{ \begin{array}{rcl} \dot{x}_1 &=& x_2 \\ \dot{x}_2 &=& -x_1^3 + \frac{1}{3}x_1 + x_2(y + 3x_1 + x_1^2) - 0.1y - 0.14 \\ \dot{y} &=& \epsilon(x_1 + 0.2). \end{array} \right. \tag{3.1}$$

3.2. Parabolic bursting

The transitions both from steady state to oscillatory state and backward occur through saddle-node homoclinic bifurcations. The spiking frequency is low at both the beginning and the end of active phase, which motivates the name *parabolic* bursting. See Fig 1.B. Unlike square-wave bursting, the parabolic bursting model in Fig 2.B has no bistability, but requires a slow variable with its own oscillation. In the model, there are two disjoint intervals in $\phi \in S^1$ for which fast subsystem is either in a steady or in an oscillatory state and they are separated at the saddle-node homoclinic bifurcation points. Bursting occurs when the slow variable moves periodically between the two intervals.

A well-known example of parabolic bursting is found in the Aplysia R-15 neuron ([1, 18]). The following system of differential equations give rise to parabolic bursting ([8]).

$$\left\{ \begin{array}{rcl} \dot{\theta} &=& 1 - \cos\theta + (1 + \cos\theta) r(\phi) \\ \dot{\phi} &=& \epsilon, \end{array} \right. \tag{3.2}$$

where $\theta \times \phi \in S^2$ and $r : S^1 \to R$ determines the intervals of ϕ for which θ is continuously spiking or in a steady state.

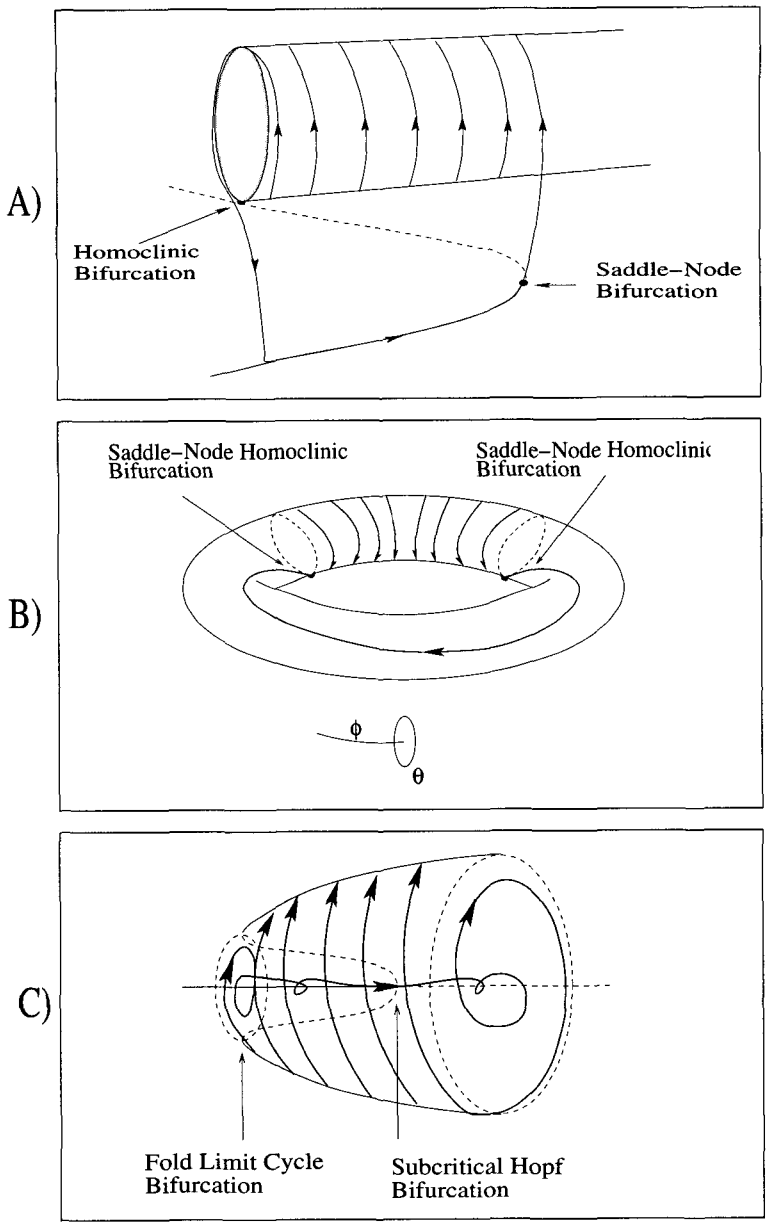

FIGURE 2. The bifurcation structures for different bursting oscillations. A: square-wave bursting, B: parabolic bursting, C: elliptic bursting.

Steady → Oscillatory / Oscillatory → Steady	Homoclinic	Saddle–Node Homoclinic	Fold Limit Cycle	Supercritical Hopf
Saddle–Node	Square–wave	Triangular		Tapered
Saddle–Node Homoclinic		Parabolic		
Subcritical Hopf			Elliptic	
Supercritical Hopf				

FIGURE 3. A classification of codimension-1 planar bursters.

3.3. Elliptic bursting

The transition from steady state to oscillatory state occurs via a subcritical Hopf bifurcation, and the spiking terminates at a fold limit cycle bifurcation as shown in Fig 2.C. We need to assume that $\dot{y} > 0$ near the branch of fixed points and $\dot{y} < 0$ near the outer branch of limit cycles. Here, the spiking amplitude gradually waxes and wanes during the active phase. This bursting is called *elliptic* because the profile of spiking amplitude resembles an ellipse as shown in Fig 1.C.

Elliptic bursting arises in models for rodent trigeminal neurons ([6]). The following system of equations give rise to elliptic bursting ([12]).

$$\begin{cases} \dot{z} &= (y+i)z + 2z|z|^2 - z|z|^4 \\ \dot{y} &= \epsilon(a - |z|^2), \end{cases} \tag{3.3}$$

where $z = x_1 + ix_2$ and $0 < a < 1$.

3.4. Classification of bursters

Besides the bursting models presented above, there are a number of other types of bursting models. Based on various bifurcation structures occurring in the transitions between steady states and oscillatory states, a comprehensive classification scheme of codimension-1 planar bursters was suggested in [12]. Fig 3 summarizes the classification scheme. In the following sections, we restrict our attention to the case of codimension-1 planar bursters. That is, the slow system is one-dimensional and the fast subsystem is two-dimensional.

4. Stability analysis

Our general method for determining the stability of periodic bursting solutions is done by constructing a two-dimensional section transverse to the flow defined by (2.1) and then considering the Poincaré return map on the section. To determine whether the return map is a contraction, we express it as the composition of several other maps. These maps are determined by the following four different pieces:

(P1) Tracking the branch of fixed points in the silent phase
(P2) Tracking the branch of limit cycles in the active phase
(P3) Transition from steady state to oscillatory state
(P4) Transition from oscillatory state to steady state

We need to estimate the amount of expansion or contraction induced by each piece. We shall show that there is a huge amount of contraction in (P1), which will easily dominate the possible expansions in (P2). Thus, the possible expansion that ultimately destroy the contraction of the entire map occur during the transitions (P3) or (P4). We now analyze each piece one by one.

4.1. The branch of fixed points

We consider the nature of flow near the branch of fixed points. Let $y = a$ and $y = b$ be the left and right bifurcation values of the branch of fixed points respectively. In order to get a bursting activity, we need to assume that the system (2.2) has an asymptotically stable fixed point $(x_*(y), y)$ for each y in the interval (a, b). This implies all the eigenvalues of $A(y) := D_x f(x_*(y), y)$ have negative real parts. Hence, it follows that the fixed point $(x_*(y), y)$ of (FS) has a domain of attraction $G(y)$ for each $y \in (a, b)$. We consider a closed interval $[y_0, y_1] \subset (a, b)$ and let $\mathcal{L}_0$ denote the branch of fixed points for y in $[y_0, y_1]$.

Introducing a slow time scale $\tau = \epsilon t$ in (2.1), we obtain an equivalent system

$$\left\{ \begin{array}{rcl} \epsilon x' & = & f(x, y) \\ y' & = & g(x, y), \end{array} \right. \tag{4.1}$$

where $'$ denotes differentiation with respect to τ. By setting $\epsilon = 0$, we have the reduced system

$$y' = g(x_*(y), y). \tag{4.2}$$

Now, the solution $(x(\tau,\epsilon), y(\tau,\epsilon))$ of (4.1) with an initial value (x_0, y_0), $x_0 \in G(y_0)$, can be approximated from the reduced system. Let the solution of (4.2) with the initial value y_0 be denoted by $\bar{y}(\tau)$. By assuming $y' > 0$ near $\mathcal{L}_0$, we have $\bar{y}(T) = y_1$ for some time $T > 0$. It follows from the classical theory of singular perturbation ([25]) that for any $\tau_\delta > 0$

$$\begin{aligned} |x(\tau,\epsilon) - x_*(\bar{y}(\tau))| &= O(\epsilon) \\ |y(\tau,\epsilon) - \bar{y}(\tau)| &= O(\epsilon) \end{aligned} \tag{4.3}$$

uniformly for $\tau_\delta \le \tau \le T$.

We now follow the geometric theory of Fenichel for a detailed analysis of the flow near $\mathcal{L}_0$. It is convenient to use the notation that $\tau \to p \cdot \tau$ indicates the solution of (4.1) with $p \cdot 0 = p$. It follows from the theory of Fenichel that the curve $\mathcal{L}_0$ perturbs smoothly to an invariant curve $\mathcal{L}_\epsilon$ for all sufficiently small $\epsilon > 0$. The distance from $\mathcal{L}_0$ to $\mathcal{L}_\epsilon$ is $O(\epsilon)$. The trajectories starting near $\mathcal{L}_\epsilon$ are attracted to $\mathcal{L}_\epsilon$ exponentially. Moreover, for each $m \in \mathcal{L}_\epsilon$, there exists a two-dimensional manifold $\mathcal{F}_\epsilon(m)$ which has the same asymptotic phase as m. We set $W_\epsilon = \cup_{m\in\mathcal{L}_\epsilon} \mathcal{F}_\epsilon(m)$. If we let $\lambda_{\max}(y)$ be the maximum of the real parts of the eigenvalues of $A(y)$ and let $-k < 0$ be a constant larger than $\lambda_{\max}(y)$ for all $y \in [y_0, y_1]$, then there is a constant C such that if $p, q \in \mathcal{F}_\epsilon(m)$, then

$$|p \cdot \tau - q \cdot \tau| \le Ce^{-k\tau}|p - q| \tag{4.4}$$

for all $\tau \ge 0$ such that $p \cdot [0,\tau] \subset W_\epsilon$ and $q \cdot [0,\tau] \subset W_\epsilon$. The family of manifolds $\{\mathcal{F}_\epsilon(m) \mid m \in \mathcal{L}_\epsilon\}$ are positively invariant, which means that

$$\mathcal{F}_\epsilon(m) \cdot \tau \subset \mathcal{F}_\epsilon(m \cdot \tau)$$

for all $m \in \mathcal{L}_\epsilon$ and all $\tau \ge 0$ such that $m \cdot [0,\tau] \subset W_\epsilon$.

We now estimate the total amount of the contraction as trajectories track $\mathcal{L}_\epsilon$. Let m_0 and m_1 be the points in $\mathcal{L}_\epsilon$ whose y-components are y_0 and y_1 respectively. Let p and q be points in $\mathcal{F}_\epsilon(m_0)$ which are $O(\epsilon)$ close to m_0. We keep track of the two trajectories starting at p and q until they arrive at $\mathcal{F}_\epsilon(m_1)$. Their arrival times are the same, and they are $O(\epsilon)$ close to T from (4.3).

We consider a regular partition of the time interval $[0, T]$

$$0 < \tau_1 < \tau_2 < \cdots < \tau_{n-1} < \tau_n = T$$

and choose a τ_i^* in $[\tau_{i-1}, \tau_i]$ for $i = 1, 2, \ldots, n$. We set $\Delta\tau = T/n$. Given a $\delta > 0$, choose $\Delta\tau$ sufficiently small. Then, it follows from (4.3) and

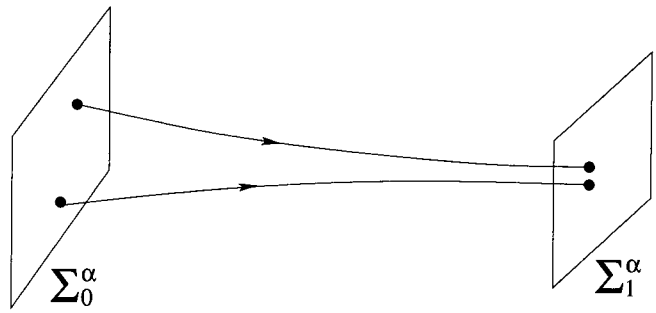

FIGURE 4. The map $\Pi_\alpha : \Sigma_0^\alpha \to \Sigma_1^\alpha$. There is a huge amount of contraction near $\mathcal{L}_\epsilon$.

(4.4) that

$$\begin{aligned} |p \cdot \tau_1 - q \cdot \tau_1| &\leq \exp[\frac{1}{\epsilon}\{\lambda_{\max}(\bar{y}(\tau_1^*)) + \delta\}\Delta\tau]|p - q| \\ &\vdots \\ |p \cdot \tau_n - q \cdot \tau_n| &\leq \exp[\frac{1}{\epsilon}\{\lambda_{\max}(\bar{y}(\tau_n^*)) + \delta\}\Delta\tau]|p \cdot \tau_{n-1} - q \cdot \tau_{n-1}|. \end{aligned}$$

Therefore,

$$|p \cdot \tau_n - q \cdot \tau_n| \leq \exp[\frac{1}{\epsilon}\sum_{i=1}^{n}\{\lambda_{\max}(\bar{y}(\tau_i^*)) + \delta\}\Delta\tau]|p - q|.$$

It is easy to see that as $n \to \infty$

$$\sum_{i=1}^{n}\{\lambda_{\max}(\bar{y}(\tau_i^*)) + \delta\}\Delta\tau \to \int_0^T \lambda_{\max}(\bar{y}(\tau))\, d\tau + T\delta.$$

Set

$$-k_1 := \int_0^T \lambda_{\max}(\bar{y}(\tau))\, d\tau < 0.$$

Thus, we have derived a formula which gives an estimate of the contraction rate near $\mathcal{L}_\epsilon$. To be more specific, let $\Sigma_0^\alpha \subset \mathcal{F}_\epsilon(m_0)$ be a local section at m_0 and $\Sigma_1^\alpha \subset \mathcal{F}_\epsilon(m_1)$ be a local section at m_1 as shown in Fig 4. Then, both sections Σ_0^α and Σ_1^α are transverse to the flow of (4.1), so the flow gives rise to a map

$$\Pi_\alpha : \Sigma_0^\alpha \to \Sigma_1^\alpha.$$

Thus, we have obtained the following result which gives a bound for the contraction rate near $\mathcal{L}_\epsilon$.

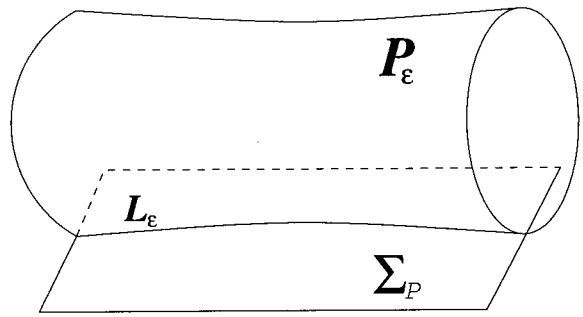

FIGURE 5. A two-dimensional section Σ_P which is transverse to $\mathcal{P}$. The section Σ_P intersects $\mathcal{P}_\epsilon$ along the curve $\mathcal{L}_\epsilon$.

PROPOSITION 1. *Let δ be any positive number. Then,*

$$|\Pi_\alpha(p) - \Pi_\alpha(q)| < e^{-\frac{k_1-\delta}{\epsilon}}|p-q|$$

for all $p,\ q \in \Sigma_0^\alpha$.

4.2. The branch of limit cycles

We now consider the nature of flow near the branch of limit cycles. Let $y = a$ and $y = b$ be the left and right bifurcation values of the branch of limit cycles respectively. We need to assume that (FS) has an asymptotically stable limit cycle $x_*(t, y)$ for each y in the interval (a, b). The stability of the limit cycle implies that one of the multipliers, denoted by $\lambda_1(y)$, of the variational equation

$$\frac{du}{dt} = D_x f(x_*(t, y), y)u$$

has its modulus less than one. We consider a closed interval $[y_0, y_1] \subset (a, b)$ and let the branch of limit cycles for $[y_0, y_1]$ be denoted by $\mathcal{P}$.

Since the manifold $\mathcal{P}$ is normally hyperbolic from our assumptions, it perturbs smoothly to an invariant manifold $\mathcal{P}_\epsilon$. Since $\mathcal{P}$ is assumed to be attracting, it follows that $\mathcal{P}_\epsilon$ is also attracting. It is now necessary to analyze the flow on the invariant manifold $\mathcal{P}_\epsilon$ and the asymptotic behaviors of the trajectories close to $\mathcal{P}_\epsilon$. It will be convenient to consider a return map defined by the flow. Let Σ_P be a two-dimensional section which is transverse to $\mathcal{P}$ as shown in Fig 5. Let

$$\Pi_P : \Sigma_P \to \Sigma_P$$

be the natural return map defined by the flow (2.1). The section Σ_P intersects $\mathcal{P}_\epsilon$ along a one-dimensional curve, which we denote by $\mathcal{L}_\epsilon$. Note that the curve $\mathcal{L}_0$ is composed of the fixed points of the map Π_P for $\epsilon = 0$.

Now, the notion of asymptotic phase in the previous section can be applied to the map Π_P exactly in the same way. That is, for each $m \in \mathcal{L}_\epsilon$, there exists a one-dimensional fiber $\mathcal{F}_\epsilon(m) \subset \Sigma_P$ that has the same asymptotic phase as m with respect to the map Π_P. Since the section Σ_P is foliated by the family of one-dimensional fibers $\{\mathcal{F}_\epsilon(m) \mid m \in \mathcal{L}_\epsilon\}$ that are positively invariant, we can find a parameterization $\mathbf{x}(u, y)$ of Σ_P satisfying $y \to \mathbf{x}(0, y)$ is a parametrization of the curve $\mathcal{L}_\epsilon$ preserving the y-th component of the points in $\mathcal{L}_\epsilon$ and $u \to \mathbf{x}(u, y)$ is a parametrization of the fiber $\mathcal{F}_\epsilon(\mathbf{x}(0, y))$ for each $y \in [y_0, y_1]$. Note that the parametrization $\mathbf{x}(u, y)$ depends on ϵ.

Now, by the parametrization, we can define a map $F_\epsilon := \mathbf{x}^{-1} \circ \Pi_P \circ \mathbf{x}$ on a subset $\mathcal{D} \subset \mathbf{R}^2$. Let

$$F_\epsilon(u, y) = (V_\epsilon(u, y), H_\epsilon(u, y)).$$

Note that $H_\epsilon(u, y)$ is independent of u from the positive invariance of the fibers $\{\mathcal{F}_\epsilon(m) \mid m \in \mathcal{L}_\epsilon\}$. Since $H_0(u, y) = y$ in $\mathcal{D}$, it is expected that we can write

$$H_\epsilon(u, y) = y + \epsilon h_\epsilon(y)$$

for some function $h_\epsilon(y)$ which is bounded with respect to ϵ. This can be shown by computing the limit

$$\lim_{\epsilon \to 0} \frac{H_\epsilon(0, y) - y}{\epsilon} = \int_0^{T(y)} g(x_*(t, y), y) dt,$$

where $T(y)$ is the period of $x_*(t, y)$. The computation is straightforward.

We now estimate the expansion rate of trajectories near $\mathcal{P}_\epsilon$. For this, choose $p_1 = (u_1, y_1)$ and $p_2 = (u_2, y_2)$ in $\mathcal{D}$ with $|u_1|$ and $|u_2|$ sufficiently small.

The Jacobian matrix of $F_\epsilon(u, y)$ at a point $(0, y) \in \mathcal{D}$ is given by

$$DF_\epsilon(0, y) = \begin{bmatrix} \frac{\partial V_\epsilon}{\partial u}(0, y) & 0 \\ 0 & 1 + \epsilon \frac{dh_\epsilon}{dy}(y) \end{bmatrix}.$$

Since $\lim_{\epsilon \to 0} |\partial V_\epsilon / \partial u(0, y)| = |\lambda_1(y)| < 1$ for all $y \in [y_0, y_1]$, there exist constants C, K such that if p_1 and p_2 are points in $\mathcal{D}$ with $|u_1|, |u_2| \leq C$, then

$$|F_\epsilon(p_1) - F_\epsilon(p_2)| \leq (1 + K\epsilon)|p_1 - p_2|,$$

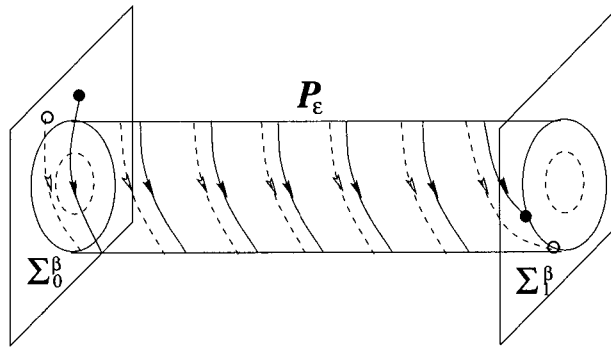

FIGURE 6. The map $\Pi_\beta : \Sigma_0^\beta \to \Sigma_1^\beta$. The expansion rate of Π_β is finite independent of ϵ.

which holds for all sufficiently small $\epsilon > 0$. Repeating this step n times, we obtain

$$|F_\epsilon^n(p_1) - F_\epsilon^n(p_2)| \ \leq \ (1 + K\epsilon)^n |p_1 - p_2|.$$

Note that there must exist a constant L (independent of ϵ) such that if $F_\epsilon^n(p_1)$ and $F_\epsilon^n(p_2)$ are in $\mathcal{D}$ after n iterations, then $n < L/\epsilon$. Hence,

$$|F_\epsilon^n(p_1) - F_\epsilon^n(p_2)| \ \leq \ (1 + K\epsilon)^{L/\epsilon} |p_1 - p_2|.$$

As $\epsilon \to 0$, the term $(1 + K\epsilon)^{L/\epsilon}$ converges to the constant $M = e^{KL}$. We conclude that

$$|F_\epsilon^n(p_1) - F_\epsilon^n(p_2)| \ \leq \ M|p_1 - p_2|. \tag{4.5}$$

Note that the constant M is independent of ϵ.

Let $\Sigma_0^\beta \subset \{y = y_0\}$ and $\Sigma_1^\beta \subset \{y = y_1\}$ be the local sections around the closed curves $\mathcal{P} \cap \{y = y_0\}$ and $\mathcal{P} \cap \{y = y_1\}$ respectively as shown in Fig. 6. Then, both sections Σ_0^β and Σ_1^β are transverse to the flow of (2.1). Now, trajectories starting at Σ_0^β are attracted immediately to $\mathcal{P}_\epsilon$ and loop around $\mathcal{P}_\epsilon$ moving slowly to the right. This continues until they intersect Σ_1^β. Thus, the flow gives rise to a map

$$\Pi_\beta : \Sigma_0^\beta \to \Sigma_1^\beta.$$

We obtain from (4.5) the following result which gives a bound on the possible expansion of the trajectories near $\mathcal{P}_\epsilon$.

PROPOSITION 2. *There exists a constant $M > 0$ such that*

$$|\Pi_\beta(p) - \Pi_\beta(q)| \leq M|p - q|$$

for any p, q in Σ_0^β.

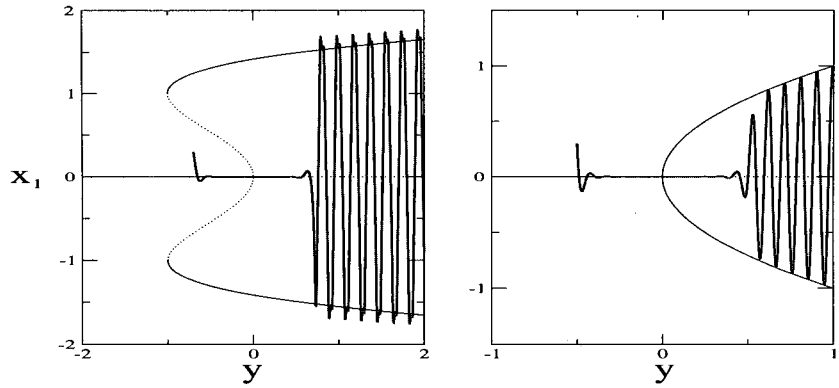

FIGURE 7. Delayed behaviors in the slow passage through Hopf bifurcations.

REMARK 1. There might be an expansion near the periodic branch, but the expansion rate is finite independent of ϵ. Thus, for sufficiently small $\epsilon > 0$, the expansion is not strong enough to break the uniform contraction of the entire return map.

4.3. Delayed behavior

We now discuss the expansion in the transitions which can ultimately break the uniform contraction of the entire map. As the trajectories pass a bifurcation point, the transition from one state to another may not be immediate, but there can be a significant delay in the transition. This phenomenon, commonly called *delayed behavior*, occurs at some of the bifurcations as trajectories make a transition from one state to another. Notice in Fig 7 that the silent phase does not end immediately after the trajectory has passed the Hopf bifurcation but that there is a significant delay ($O(1)$ in the slow time scale) before jumping to the active phase. This delayed behavior in the slow passage through Hopf bifurcation is a well-studied subject in the singular perturbation literature ([2, 17]).

If there is a delayed behavior, then a strong expansion of trajectories may occur during the transition. Note first that in order to get an expansion during the transition, there must be some branch of unstable sets at which trajectories can stay after passing the bifurcation; this branch may or not exist depending on the bifurcation structures. Moreover, we need an expansion of rate $O(e^{k/\epsilon})$ to balance the contraction of rate $O(e^{-k/\epsilon})$. The expansion rate depends on how long the trajectories

stay at the branch of unstable sets. In the next we estimate how much the trajectories can expand during the delayed time.

First, choose a compact neighborhood K of the bifurcation point containing all the fixed points, the limit cycles, and the unstable sets near the bifurcation point. Then, we may assume that the trajectories stay in K during the whole time of the transition. We now estimate how much the trajectories in K can expand for a given time.

PROPOSITION 3. *There is a constant $L > 0$ such that*

$$|p \cdot \tau - q \cdot \tau| \leq e^{\frac{L}{\epsilon}\tau}|p - q|$$

for all $p, q \in K$ and $\tau \geq 0$ such that $p \cdot [0, \tau] \subset K$ and $q \cdot [0, \tau] \subset K$.

Proof. We express the system (4.1) as

$$X' = \frac{1}{\epsilon}F(X, \epsilon), \tag{4.6}$$

where $X = (x, y)$ and $F(X, \epsilon) = (f(X), \epsilon g(X))$. Since $F(X, \epsilon)$ is $O(1)$ with respect to ϵ, we can find a Lipschitz constant $L > 0$ and an $\epsilon_0 > 0$ such that if $\epsilon < \epsilon_0$, then

$$|F(p, \epsilon) - F(q, \epsilon)| \leq L|p - q|$$

for all p, q in K. By integrating (4.6), we obtain

$$p \cdot \tau - q \cdot \tau = p - q + \int_0^\tau \frac{1}{\epsilon}\{F(p \cdot s, \epsilon) - F(q \cdot s, \epsilon)\}\, ds.$$

Then,

$$|p \cdot \tau - q \cdot \tau| \leq |p - q| + \int_0^\tau \frac{L}{\epsilon}|p \cdot s - q \cdot s|\, ds. \tag{4.7}$$

Applying Gronwall's inequality to (4.7) gives

$$|p \cdot \tau - q \cdot \tau| \leq |p - q|e^{\frac{L}{\epsilon}\tau}.$$

The proof is now complete. □

REMARK 2. It follows that in order to get an expansion of rate $O(e^{k/\epsilon})$ for some $k > 0$, trajectories need an expansion time of $O(1)$ in the slow time scale.

4.4. Transition from steady state to oscillatory state

The analysis of the bifurcation structures involved in the transition from steady state to oscillatory state shows that delayed behaviors occur in both supercritical and subcritical Hopf bifurcations ([17]). As for the other bifurcations in Fig 3, there does not exist a branch of unstable sets at which the trajectories can stay after passing the bifurcation point.

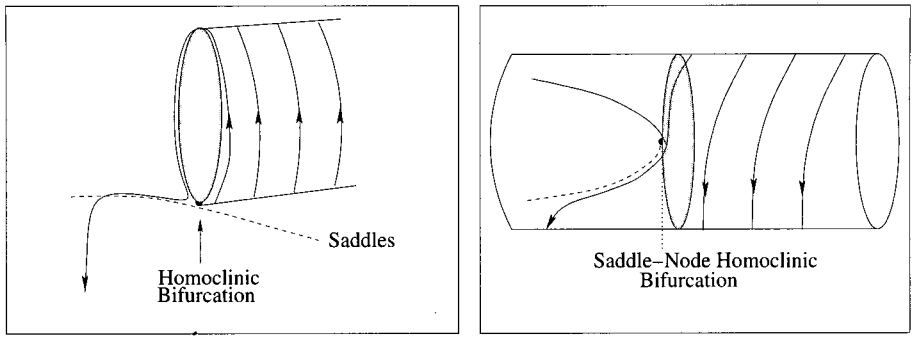

FIGURE 8. Delayed behaviors in the transition from oscillatory state to steady state.

4.5. Transition from oscillatory state to steady state

Delayed behavior may also occur at a homoclinic bifurcation or a saddle-node homoclinic bifurcation. After passing the bifurcation point, some trajectories may remain close to the saddle branch for some finite time (slow time) before attracted to the branch of stable fixed points. See Fig 8. However, there is a significant difference between the delayed behaviors through the homoclinic (saddle-node homoclinic) bifurcation and those through the Hopf bifurcations. If we consider a local section Σ at the periodic branch (like the section Σ_1^β in Fig 6) which is $O(1)$ distant from the homoclinic (saddle-node homoclinic) bifurcation, then the set of points in Σ whose trajectories have a delayed time (slow time) longer than a $\delta > 0$ is a very small subset of Σ. This explains the reason why the delayed behaviors through homoclinic (saddle-node homoclinic) bifurcations are rarely observed in the numerical simulations. See [14, 15] for the rigorous mathematical analysis of this behavior. We shall call this type of delayed behavior a *rare delayed behavior* in contrast to the *usual delayed behavior* in the Hopf bifurcations. As for the other bifurcations in Fig. 3, there does not exist a branch of unstable sets at which the trajectories can stay after passing the bifurcation point.

REMARK 3. We will be more precise about our definition of 'no delayed behavior' at a bifurcation in a transition from one state to another, since our main result below holds for the case: Fix a y_0 which is not in the bifurcation. Then, for any small $\tau_\delta > 0$, there are positive constants C_1, C_2, and τ_1 (work for all sufficiently small ϵ) such that any trajectory which starts at a point whose y-th component is y_0 and lies in the $C_1\epsilon$

neighborhood of one state will stay in the $C_1\epsilon$ neighborhood of the state for $0 \leq \tau \leq \tau^* - \tau_\delta$ and will be in the $C_2\epsilon$ neighborhood of the other state for $\tau^* + \tau_\delta \leq \tau \leq \tau_1$, where τ^* is the moment when the trajectory crosses the bifurcation.

5. Main result

We now put together all the information obtained in the previous sections. In the branch of fixed points there is a strong contraction of rate $O(e^{-k_0/\epsilon})$ for some $k_0 > 0$, which can easily overpower the possible expansion of the branch of limit cycles for small ϵ, since the expansion rate is finite independent of ϵ. During transitions, in order to get an expansion of $O(e^{k_0/\epsilon})$, trajectories need an expansion time of $O(1)$ in the slow time scale. We have also obtained a bound of the expansion rate for a given expansion time.

We next draw a conclusion from these information. Suppose that there is no delayed behavior in a burster. Then, we set y_0 and y_1 at the branch of fixed points to be sufficiently close to the bifurcations on its left and its right respectively and construct the local sections Σ_0^α and Σ_1^α, which was defined in Section 4.1. In a similar fashion, we construct the local sections Σ_0^β and Σ_1^β at the branch of limit cycles. Then, we have a flow-defined map

$$\Pi_{\alpha\beta} : \Sigma_1^\alpha \to \Sigma_0^\beta$$

in the transition from steady state to oscillatory state, and a flow-defined map

$$\Pi_{\beta\alpha} : \Sigma_1^\beta \to \Sigma_0^\alpha$$

in the transition from oscillatory state to steady state. The maps $\Pi_{\alpha\beta}$ and $\Pi_{\beta\alpha}$ are both well-defined. This comes from our assumption there is no delayed behavior at the bifurcations.

Let $\Pi = \Pi_{\beta\alpha} \circ \Pi_\beta \circ \Pi_{\alpha\beta} \circ \Pi_\alpha$. Then, we have a Poincaré return map

$$\Pi : \Sigma_0^\alpha \to \Sigma_0^\alpha.$$

The constant $k > 0$ in the expansion rate $e^{k/\epsilon}$ of the map $\Pi_{\alpha\beta}$ or $\Pi_{\beta\alpha}$ can be made arbitrarily small by taking y_0 and y_1 sufficiently close to the bifurcations. Hence, the entire map Π must be a contraction. It follows that the periodic bursting solution is asymptotically stable. We summarize this result in the following theorem.

Steady → Oscillatory / Oscillatory → Steady	Homoclinic	Saddle–Node Homoclinic	Fold Limit Cycle	Supercritical Hopf
Saddle–Node	Type II	Type II	Type I	Type I
Saddle–Node Homoclinic	Type II	Type II	Type I	Type I
Subcritical Hopf	Type III	Type III	Type III	Type III
Supercritical Hopf	Type III	Type III	Type III	Type III

FIGURE 9. A classification of the codimension-1 planar bursters according to their delayed behaviors.

THEOREM 4. *In the planar codimension-1 bursters which have no delayed behavior, the periodic bursting solution is asymptotically stable for all sufficiently small* $\epsilon > 0$.

Since the stability of bursting models is directly connected with their delayed behaviors, we classify the codimension-1 planar bursters according to their delayed behaviors. The different stability types are:

- **Type I**: there is no delayed behavior in the transitions.
- **Type II**: there is only a rare delayed behavior in the transitions.
- **Type III**: there is a usual delayed behavior in the transitions.

Fig 9 summarizes the classification, which follows from the analysis of the bifurcation structures in the previous sections. Bursters in two different groups show fundamentally different stability behaviors (see the remarks below). As for the stability type I bursters, we can characterize the set of the parameters ϵ for which the periodic bursting solution is stable.

COROLLARY 5. *As for the four bursters which are of stability type I, the periodic bursting solution is asymptotically stable for all sufficiently small* $\epsilon > 0$.

REMARK 4. In the case of stability type II bursters, even though it is rare, it is possible that the expansion during transitions can overpower the contraction of the branch of fixed points. We can characterize the parameter values of ϵ for which the periodic bursting solution is stable. The results in [8], [14], and [15] suggest that the periodic bursting solution in this group is asymptotically stable except for those in a sequence of intervals $(\epsilon_i - \delta_i, \epsilon_i + \delta_i)$, where $\epsilon_i \to 0$ as $i \to \infty$. Moreover, $\delta_i \leq e^{-k/\epsilon_i}$

and $\epsilon_i - \epsilon_{i+1} \geq C\epsilon_i^2$ for some positive constants k and C. Each interval corresponds to the parameter values of ϵ for which the model makes a transition from n to $n+1$ spikes per burst. The bursting solutions can be chaotic for these parameter values of ϵ. ([23, 24])

REMARK 5. The bursters of stability type III seem to the toughest cases for the stability analysis. For example, the elliptic burster is notorious for its instability. The primary factor which contributes to the instability of type III bursters seems to be the expansion in the transitions which may overpower the contraction of the branch of fixed points.

References

[1] W. B. Adams and J. A. Benson, *The generation and modulation of endogenous rhythmicity in the aplysia bursting pacemaker neurone R15*, Progr. Biophys. Molec. Biol. **46** (1985), 1–49.

[2] S. M. Baer, T. Erneux, and J. Rinzel, *The slow passage through a Hopf bifurcation: delay, memory effects, and resonances*, SIAM J. Appl. Math. **49** (1989), 55–71.

[3] R. Bertram, M. J. Butte, T. Kiemel, and A. Sherman, *Topological and phenomenological classification of bursting oscillations*, Bull. Math. Biol. **57** (1995), 413–439.

[4] R. J. Butera, J. Rinzel, and J. C. Smith, *Models of respiratory rhythm generation in the pre-Botzinger complex: I. Bursting pacemaker model*, J. Neurophysiology **82** (1999), 382–397.

[5] T. R. Chay and J. Keizer, *Minimal model for membrane oscillations in the pancreatic β-cell*, Biophys. J. **42** (1983), 181–190.

[6] C. A. Del Negro, C. F. Hsiao, S. H. Chandler, and A. Garfinkel, *Evidence for a novel bursting mechanism in rodent trigeminal neurons*, Biophys. J. **75** (1998), 174–182.

[7] G. de Vries, *Multiple bifurcations in a polynomial model of bursting oscillations*, J. Nonlinear Sci. **8** (1998), 281-316.

[8] G. B. Ermentrout and N. Kopell, *Parabolic bursting in an excitable system coupled with a slow oscillation*, SIAM J. Appl. Math. **46** (1986), 233–253.

[9] N. Fenichel, *Geometric singular perturbation theory for ordinary differential equations*, J. Differential Equations **31** (1979), 53–98.

[10] M. Golubitsky, K. Josic, and T. J. Kaper, *An unfolding theory approach to bursting in fast-slow systems*, In: Global Analysis of Dynamical Systems (H.W. Broer, B. Krauskopf and G. Vegter, eds.), Institute of Physics Publ. (2001), 277-308.

[11] J. Guckenheimer and P. J. Holmes, *Nonlinear Oscillations, Dynamical Systems, and Bifurcations of Vector Fields*, Springer-Verlag, New York, 1983.

[12] E. M. Izhikevich, *Neural excitability, spiking and bursting*, Inter. J. Bifur. Chaos **10** (2000), no. 6, 1171–1266.

[13] Y. A. Kuznetsov, *Elements of applied bifurcation theory*, Springer-Verlag, New York, 1995.

[14] E. Lee, *Stability analysis of parabolic bursting*, In preparation.

[15] E. Lee and D. Terman, *Uniqueness and stability of periodic bursting solutions*, J. Differential Equations **158** (1999), 48–78.

[16] C. Morris and H. Lecar, *Voltage oscillations in the barnacle giant muscle fiber*, Biophys. J. **35** (1981), 193–213.

[17] A. Nejshtadt, *Asymptotic investigation of the loss of stability by an equilibrium as a pair of eigenvalues slowly cross the imaginary axis*, Uspekhi Mat. Nauk **40** (1985), 190–191.

[18] R. E. Plant and M. Kim, *On the mechanism underlying bursting in the Aplysia abdominal ganglion R-15 cell*, Math. Biosci. **26** (1975), 357–375.

[19] J. Rinzel, *A formal classification of bursting mechanisms in excitable systems*, In: Proceedings of the International Congress of Mathematicians, vol. 1 & 2 (pp. 1578–1593). American Mathematical Society, Providence, RI, 1987.

[20] J. Rinzel and Y. S. Lee, *On different mechanism for membrane potential bursting*, In: Lecture Notes in Biomathematics, vol. 66 (pp. 19–33). Springer-Verlag, New York, 1986.

[21] J. Rubin and D. Terman, *Geometric singular perturbation analysis of neuronal dynamics*, In: Handbook of Dynamical Systems, vol.3: Towards Applications, Elsevier, 2002.

[22] A. Sherman, J. Rinzel, and J. Keizer, *Emergence of organized bursting in clusters of pancreatic β-cells by channel sharing*, Biophys. J. **54** (1988), 411–425.

[23] D. Terman, *Chaotic spikes arising from a model for bursting in excitable membranes*, SIAM J. Appl. Math. **51** (1991), 1418–1450.

[24] ———, *The transition from bursting to continuous spiking in excitable membrane models*, J. Nonlinear Sci. **2** (1992), 135–182.

[25] A. N. Tihonov, *On the dependence of the solutions of the differential equations on a small parameter*, Mat. Sb. **31** (1948), 575–586.

Department of Mathematics
Soongsil University
Seoul 156-743, Korea
E-mail: ewlee@ssu.ac.kr